

Journal of Materials Chemistry B

Accepted Manuscript



This is an *Accepted Manuscript*, which has been through the Royal Society of Chemistry peer review process and has been accepted for publication.

Accepted Manuscripts are published online shortly after acceptance, before technical editing, formatting and proof reading. Using this free service, authors can make their results available to the community, in citable form, before we publish the edited article. We will replace this *Accepted Manuscript* with the edited and formatted *Advance Article* as soon as it is available.

You can find more information about *Accepted Manuscripts* in the [Information for Authors](#).

Please note that technical editing may introduce minor changes to the text and/or graphics, which may alter content. The journal's standard [Terms & Conditions](#) and the [Ethical guidelines](#) still apply. In no event shall the Royal Society of Chemistry be held responsible for any errors or omissions in this *Accepted Manuscript* or any consequences arising from the use of any information it contains.

Coumarin dye-embedded semiconducting polymer dots for ratiometric sensing of fluoride ions in aqueous solution and bioimaging in cells†

Ya-Chi Huang, Chuan-Pin Chen, Pei-Jing Wu, Shih-Yu Kuo, and Yang-Hsiang Chan*

Received (in XXX, XXX) Xth XXXXXXXXXX 201X, Accepted Xth XXXXXXXXXX 201X

First published on the web Xth XXXXXXXXXX 201X

DOI: 10.1039/b000000x

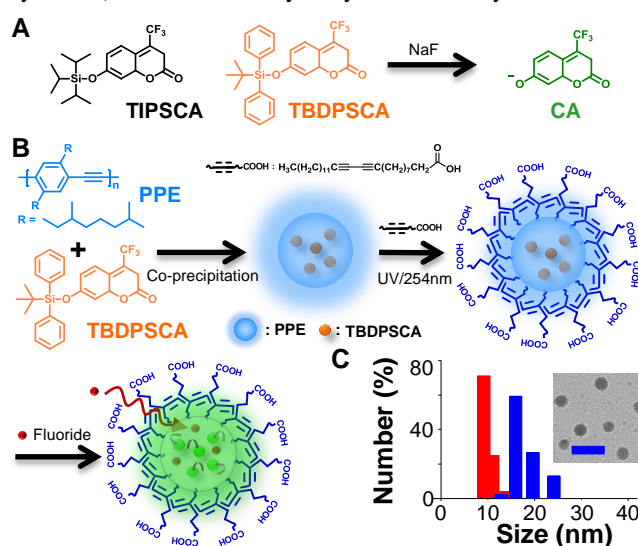
This paper describes a simple platform that employs coumarin dye-encapsulated semiconducting polymer dots as a fluorescent probe for ratiometric and sensitive fluoride anion detection, in which the sensing mechanism is based on the deprotection of the *tert*-butyldimethylsilyl group on coumarin to induce Förster resonance energy transfer.

The detection of biologically relevant anions has attracted increasing interest due to their pivotal importance in physiological and chemical processes.¹ Among these anions, fluoride is one of the most important targets because it is associated with numerous human diseases and nerve gases. Fluoride is voluntarily added to drinking water systems in many communities in an effort to promote dental health and has also been used for the treatment of osteoporosis. Excessive amounts of fluoride, however, can cause fluorosis which leads to osteosarcoma, urolithiasis, or even cancer.² The U.S. Environmental Protection Agency sets an enforceable drinking water regulation for fluoride with a maximum contaminant level at 4.0 ppm (95 μ M).³ As a result, substantial efforts have been devoted to the development of better sensors for the detection of fluoride.^{4–8} Among them, while most of the reports could only be used for the recognition of fluoride in a tetrabutylammonium fluoride salt in organic solvents or in organic-aqueous mixtures,^{5–7} there has been a paucity of studies that can be applied for the detection of fluoride, particularly NaF, in 100% aqueous solutions.⁸ Therefore, the exploration of novel probes for the selective evaluation of fluoride ions in aqueous media for biological and environmental studies remains highly desirable.

In the past few years, nanoparticle-based assemblies have emerged as a new type of ion sensors because of their good sensitivity and selectivity, simplicity, high reliability, and relatively low cost.^{9–11} Recently, semiconducting polymer nanoparticles (Pdots) have attracted enormous interest due to their excellent characteristics, including extraordinary fluorescence brightness, fast radiative rate, good photostability, and low cytotoxicity.^{12–14} Moreover, the facile surface functionalization of Pdots allows them to be widely used for various applications both *in vitro* and *in vivo*.^{15,16} Very recently, Chiu's group has developed various sensing platforms by taking advantage of the amplified energy transfer from the excited Pdot matrices to the fluorescent sensing probes (e.g. pH- or temperature-sensitive dyes).^{17,18}

In this communication, we report a novel strategy for the ratiometric detection of fluoride ions in 100% water. Ratiometric measurement has several advantages in which it is

minimally affected by the fluctuation of the excitation source, probe concentration, and drifts in the instrument/environment. Specifically, we first synthesized triisopropylsilyl (TIPS)- and *tert*-butyldiphenylsilyl (TBDPS)-protected 7-hydroxy-4-trifluoromethyl coumarin (Scheme 1A, see ESI† for detailed synthesis) in which the hydroxyl functionality of coumarin



Scheme 1. Schematic showing the sensing of fluoride using coumarin dye-doped PPE Pdots. (A) Molecular structures of TIPSCA and TBDPSCA, and the sensing mechanism for the detection of NaF. (B) Semiconducting polymer, PPE, and TBDPSCA dyes were mixed together in THF and then co-precipitated in water under vigorous sonication conditions to form TBDPSCA-embedded PPE Pdots. The Pdots were further coated with a layer of polydiacetylenes (PDAs) to prevent the potential leakage of the trapped CA dyes. Yet small fluoride ions could permeate into the Pdot matrix to deprotect the silyl group of TBDPSCA, making CA highly fluorescent due to energy transfer from PPE to CA. (C) Hydrodynamic diameters of CA-doped PPE Pdots before (red histograms) and after (blue histograms) the assembly of PDAs. The inset shows the TEM image of PDA enclosed Pdots. The scale bar represents 100 nm.

(CA) was protected so that the molecules exhibited no fluorescence. We expected that the treatment of fluoride could rapidly and efficiently deprotect the TIPS/TBDPS group on CA. In this strategy (Scheme 1B), we first blended TIPSCA/TBDPSCA with poly(2,5-di(3',7'-dimethyloctyl)phenylene-1,4-ethynylene) (PPE) in THF. The mixtures of TIPSCA/TBDPSCA and PPE were then injected into water by nanoprecipitation under vigorous sonication. This sudden change of solvent environment, along with vigorous sonication, led to the formation of coumarin-doped

Pdots of ~9 nm in diameter (Scheme 1C). However, we found that the TIPSCA-embedded PPE Pdots showed strong fluorescence immediately upon the exposure to water during Pdot preparation. This phenomenon indicated that the Si-O bond of TIPS was subjected to cleavage through the interactions with water molecules. On the other hand, the TBDPS moiety exhibited better stability under aqueous solutions, which allowed us to proceed to the fluoride driven silyl deprotection (*vide infra*). To prevent the potential leaching of CA from Pdot matrix and at the same time provide the functionality of Pdots for further bioconjugation, we enclosed carboxyl-functionalized diacetylenes (10,12-pentacosadiynoic acid) onto the surface of Pdots, followed by the polymerization of diacetylenes via topochemical 1,4-addition.¹⁹ We then purified the resulting Pdots through centrifugal filtration device (Amicon® Ultra-4, MWCO: 100 kDa) to remove the free TBDPS and DAs. As shown in Scheme 1D, the average diameter of Pdots increased from 9 to 17 nm after the capping of polydiacetylenes (PDAs), suggesting that only a monolayer of PDAs was assembled onto the surface of each single Pdot. Besides, the appearance of a new peak at 650 nm in the absorption spectrum (red line, Fig. 1A) also demonstrated the formation of highly ordered blue-phase PDA assemblies on Pdots.¹⁹

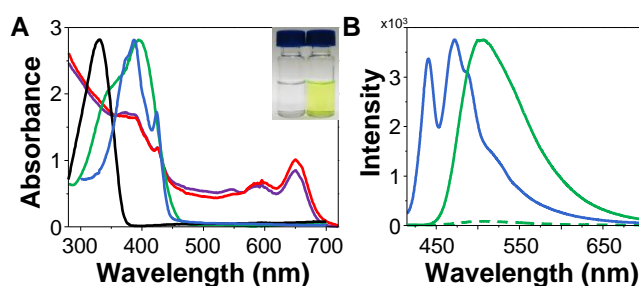


Figure 1. (A) UV-visible spectra of PPE Pdots in water (blue line), TBDPSCA in methanol (black line), CA in methanol (green line), upon the addition of NaF), PDA-capped PPE/TBDPSCA Pdots in water (red line), and PDA-capped PPE/CA Pdots in water (purple line, after the addition of NaF). The inset in the upper-right corner shows the photographs of TBDPSCA solution in methanol before (left image) and after the addition of NaF (right image). (B) Emission spectra of PPE Pdots in water (blue line), TBDPSCA in methanol (dashed green line), and CA in methanol (solid green line, upon the addition of NaF) with $\lambda_{\text{ex}} = 405$ nm.

Fig. 1A shows the UV-visible absorption of TBDPSCA before (black line) and after (green line) treatment with NaF in methanol. Addition of fluoride anions cleaved the TBDPS group that resulted in a prompt color change of TBDPSCA solution from colorless to yellow (upper-right inset in Fig. 1A). The accompanying emergence of a new strong absorption band centered at 400 nm allowed us to design a Förster resonance energy transfer (FRET) based fluoride sensing due to the extensive spectral overlap between the emission of PPE and the absorption of CA. Consequently, upon the addition of fluoride, we expected that the fluorescence of PPE was quenched while the emission of CA was enhanced due to energy transfer from PPE to CA, thereby allowing us to apply ratiometric ion determination based on two fluorescence emission intensities. The emission spectra of PPE, TBDPSCA, and CA were shown in Fig. 1B.

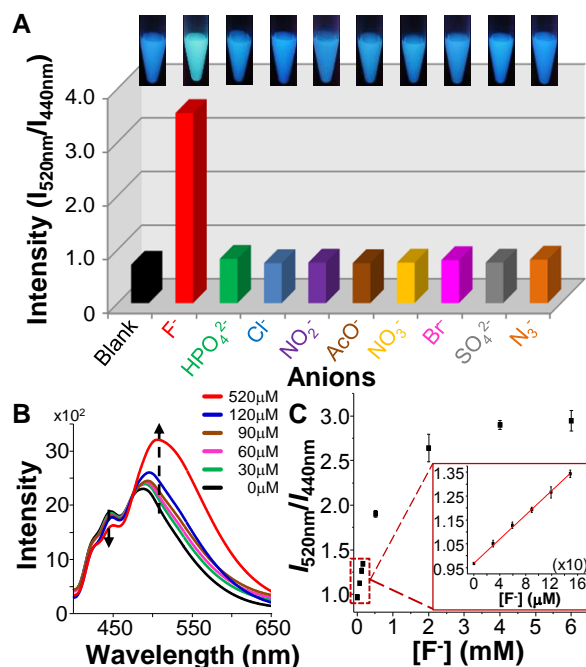


Figure 2. (A) Effects of different ions (25 mM) on the fluorescence intensity of solutions containing PDA-coated PPE/TBDPSCA Pdots. Images on the top show each sample under a 365 nm lamp. (B) Effect of various concentrations of F^- on the fluorescence of solutions containing PDA-coated PPE/TBDPSCA Pdots. Concentrations of F^- ranged from 0–160 μM (0–6.7 ppm) at $\lambda_{\text{ex}} = 405$ nm. Concentration of Pdots used was 30 nM at pH 6.7. (C) A plot of the ratio of the 520 nm peak (from CA) over the 440 nm peak (from PPE Pdots) as a function of F^- concentration. The red line is a linear fit to the data ($R^2 = 0.9992$). The inset in (C) magnifies the regions of lower concentrations of F^- (<160 μM).

Besides F^- , we have examined the effect of various other anions on the fluorescence ratio of PPE to CA (Fig. 2A), and found that their emission ratio was unaffected or minimally affected by other anions, as compared with the emission ratio of PPE to CA in pure water (Blank). We also examined the interference effect of mixed anions by measuring the fluorescence emission of PPE and CA in the mixture of anions containing NO_2^- , Cl^- , AcO^- , and NO_3^- . We found that negligible change of PPE and CA emission was observed in the absence of F^- . An increased fluorescence of CA along with a concomitant decrease of PPE emission appeared when F^- was added into the mixture (Fig. S1, ESI†). Fig. 2B shows the emission spectra of solutions containing PDA-enclosed TBDPSCA-doped PPE Pdots as a function of F^- concentration. It is evident that while the emission intensity of CA (520 nm) increased, the PPE Pdots decreased their intensity (440 nm) with increasing F^- concentrations. For this set of experiments, the relative standard deviation of blank signal from 10 replicates was 0.6%. An increased signal of ~5% from CA emission accompanied by a quenching signal of ~2% from PPE emission could be observed at 15 μM of fluoride ions. Fig. 2C shows a linear correlation between the ratio of $I_{520\text{nm}}/I_{440\text{nm}}$ and F^- concentration, ranging from 0 μM to 160 μM ($R^2 = 0.9992$).

The ratiometric changes of PPE and CA emission can be explained using a FRET model, a nonradiative dipole-dipole interaction. Upon the addition of F^- , the TBDPS protecting

groups were cleaved and the deprotected CA became emissive via FRET mechanism. The Förster radius R_o can be calculated from:

$$R_o^6 = 8.79 \times 10^{-5} (\kappa^2 n^{-4} Q_D J) \quad (\text{in } \text{Å}) \quad (1)$$

R_o is the Förster-like radius that represents a specific separation distance where the energy transfer efficiency is reduced to 50% of the maximal value. κ^2 is an orientation factor, which is set to 2/3 for a randomly orientated donor-acceptor pair in solution. n is the refractive index of the medium, which is assumed to be 1.6 in average for a general poly(phenylene ethynylene) polymer. Q_D is the quantum yield of the donor in the absence of acceptors, which is 12% for PPE Pdots. J is the spectral integral as a function of wavelength and expresses the degree of spectral overlap between the emission spectrum of the donor and the absorption spectrum of the acceptor, which can be calculated using equation S1 (see ESI†). Based on this information, the Förster radius, R_o , was determined to be 2.9 nm using equation 1. We also calculated the FRET efficiency (> 99%) and compared with the experimental values (58-61%, see ESI†), in which the difference might be ascribed to the uneven distribution of coumarin dyes inside Pdots or the hydrophobic nature of Pdot core that could prevent the fluoride ions from penetrating the interior of the Pdots.

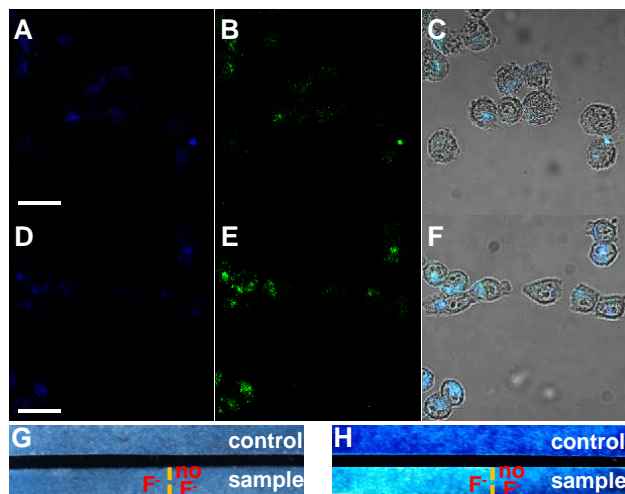


Figure 3. Confocal microscopy images of live HeLa cells labeled by Pdots before (A-B) and after (D-E) the incubation with 25 mM NaF for 2 h at 37 °C. Their corresponding fluorescence overlaid with the bright-field images are shown in (C) and (F), respectively. The blue channels shown in (A) and (D) were produced by integrating the spectral region from 433 to 467 nm, while the green channels shown in (B) and (E) were from 500 to 530 nm. The scale bars are 20 μm. Color changes of test paper containing PDA-enclosed TBDPSCA-PPE Pdots after immersion into 1 mM NaF for 30 s, under (G) ambient light or (H) 365nm UV light.

We further applied this Pdot-based sensor for detection of F^- in live HeLa cells. The TBDPSCA-doped PPE Pdots were introduced into cells via endocytosis and then a NaF solution was added into the cell-culture medium to reach a final concentration of 25 mM. After incubation with NaF for 2 h, we washed the cells with PBS buffer to remove free Pdots in solution and on the cell surface. Fig. 3A shows the confocal

fluorescence microscopy images of HeLa cells before (A-C) and after (D-F) the addition of NaF. It clearly shows that the emission intensity of CA (green fluorescence) increased after the treatment of NaF while the emission intensity of PPE decreased slightly (blue fluorescence), which is consistent with the spectral response (Fig. 2). We also evaluated the feasibility of this sensing system in environmental conditions. Here we used Hardness WasteWatR™ (#507 ERA, CO, USA)²⁰ to simulate environmental fluids and at the same time served as a controlled solution. The simulated samples were prepared by spiking 90 μM of F^- into Hardness WasteWatR™ solution containing the Pdot sensors. We then estimated the F^- concentration from the ratio of I_{520nm}/I_{440nm} . This measurement showed that the concentration of F^- was $84.98 \pm 5.78 \mu\text{M}$. For simulated physiological samples, we spiked 90 μM NaF into RPMI-1640 cell culture solutions (Table S1) and the estimated F^- concentration was $93.24 \pm 1.14 \mu\text{M}$, which exhibited a good agreement with the spiking value. We also prepared a test stripe impregnated with Pdots and then immersed it into a solution containing F^- , where obvious green fluorescence appeared immediately (Fig. 3B).

In conclusion, we have developed a selective, sensitive, and ratiometric approach for F^- detection in aqueous media based on coumarin-doped Pdot sensors. The linear detection range for F^- falls within the ecotoxicologically (environmentally) relevant concentration range. This simple, sensitive, and economical technique takes advantage of the high brightness and optical tunability of Pdots, and affords a means of rapid determination of F^- for biological or environmental analysis.

Notes and references

Department of Chemistry, National Sun Yat-sen University, Kaohsiung, Taiwan. Fax: 011-886-7-3684046; Tel: 011-886-7-5252000 ext. 3921; E-mail: yhchan@mail.nsysu.edu.tw

† Electronic Supplementary Information (ESI) available: Synthesis of coumarin dyes and experimental section. See DOI: 10.1039/b000000x/

- Martínez-Máñez, R.; Sancenón, F. *Chem. Rev.* **2003**, *103*, 4419.
- Bassin, E. B.; Wypij, D.; Davis, R. B. *Cancer Causes Control* **2006**, *17*, 421.
- <http://water.epa.gov/action/advisories/drinking/upload/dwstandards2012.pdf>, Assessed January 09, 2014
- Cametti, M.; Rissanen, K. *Chem. Commun.* **2009**, 2809.
- E.J.Cho; J.W.Moon; S.W.Ko; J.Y.Lee; Kim, S. K.; Yoon, J.; Nam, K. C. *J. Am. Chem. Soc.* **2003**, *125*, 12376.
- Guha, S.; Saha, S. *J. Am. Chem. Soc.* **2010**, *132*, 17674.
- Wade, C. R.; Ke, I.-S.; Gabbaï, F. P. *Angew. Chem. Int. Ed.* **2012**, *51*, 478.
- Kim, S. Y.; Park, J.; Koh, M.; Park, S. B.; Hong, J.-I. *Chem. Commun.* **2009**, 4735.
- Lin, S.-Y.; Wu, S.-H.; Chen, C.-h. *Angew. Chem. Int. Ed.* **2006**, *118*, 5044.
- Lan, G.-Y.; Huang, C.-C.; Chang, H.-T. *Chem. Commun.* **2010**, *46*, 1257.
- Chan, Y.-H.; Chen, J.; Liu, Q.; Wark, S. E.; Son, D. H.; Batteas, J. D. *Anal. Chem.* **2010**, *82*, 3671.
- Wu, C.; Bull, B.; Szymanski, C.; Christensen, K.; McNeill, J. *ACS Nano* **2008**, *2*, 2415.
- Li, K.; Liu, B. *J. Mater. Chem.* **2012**, *22*, 1257.
- Wu, C.; Chiu, D. T. *Angew. Chem. Int. Ed.* **2013**, *52*, 3086.
- Wu, C.; Jin, Y.; Schneider, T.; Burnham, D. R.; Smith, P. B.; Chiu, D. T. *Angew. Chem., Int. Ed.* **2010**, *49*, 9436.
- Wu, P.-J.; Chen, J.-L.; Chen, C.-P.; Chan, Y.-H. *Chem. Commun.* **2013**, *49*, 898.
- Chan, Y.-H.; Wu, C.; Ye, F.; Jin, Y.; Smith, P. B.; Chiu, D. T. *Anal. Chem.* **2011**, *83*, 1448.

- 18 Ye, F.; Wu, C.; Jin, Y.; Chan, Y.-H.; Zhang, X.; Chiu, D. T. *J. Am. Chem. Soc.* **2011**, *133*, 8146.
- 19 Yarimaga, O.; Jaworski, J.; Yoon, B.; Kim, J.-M. *Chem. Commun.* **2012**, *48*, 2469.
- 5 20. <http://www.eraqc.com/DesktopModules/ERAMSDS/ViewPDF.aspx?id=d5067f1c-7fe4-45e4-8225-0129a39b32b2>

TOC Graphic

10 This communication demonstrates a simple platform for using coumarin-encapsulated Pdots as a sensor for ratiometric determination of fluoride ions

